The Hexadentate Ligand 1,4,7-Tris(*o*-aminobenzyl)-1,4,7-triazacyclononane and Its Complexes with Zinc(II), Cadmium(II), and Mercury(II) in Solution and in the Solid State

Oliver Schlager,[1a] Karl Wieghardt,*[,1a] Hiltrud Grondey,[†,1b] Anna Rufińska,[1b] and Bernhard Nuber[1c]

Max-Planck-Institut für Strahlenchemie, D-45470 Mülheim, Germany, Max-Planck-Institut für Kohlenforschung, D-45470 Mülheim, Germany, and Anorganisch-Chemisches Institut der Universität, D-69120 Heidelberg, Germany

Received June 1, 1995[⊗]

The new hexadentate ligand 1,4,7-tris(*o*-aminobenzyl)-1,4,7-triazacyclononane (L) has been prepared from the reaction of 1,4,7-triazacyclononane and 2-nitrobenzyl bromide (1:3) in toluene and subsequent reduction of 1,4,7-tris(*o*-nitrobenzyl)-1,4,7-triazacyclononane with hydrazine hydrate and a graphite catalyst. The ligand forms stable complexes with the salts $M(ClO_4)_2 \cdot 6H_2O$ in methanol ($M = Zn^{2+}$, Cd^{2+}, Hg^{2+}). The complexes $[LZn](ClO_4)_2$, **1**, $[LCd](ClO_4)_2 \cdot 0.5H_2O$, **2**, and $[LHg](ClO_4)_2 \cdot 0.5H_2O$, **3**, have been isolated, and their solid state structures have been determined by X-ray single-crystal crystallography. Complex **1**, $[Zn(C_{27}H_{36}N_6)](ClO_4)_2$, crystallizes in the monoclinic space group $P2_1/n$ with $Z = 4$, $a = 9.222(5)$ Å, $b = 17.01(1)$ Å, $c = 19.41(1)$ Å, and $\beta = 97.03(5)°$; **2** and **3** (data in parentheses), $[Cd(C_{27}H_{36}N_6)](ClO_4)_2 \cdot 0.5H_2O$ and $[Hg(C_{27}H_{36}N_6)](ClO_4)_2 \cdot 0.5H_2O$, crystallize in the orthorhombic space group $Pc2_1n$, which is a nonstandard setting of $Pna2_1$ (No. 33), with $Z = 4$, $a = 10.882(2)$ Å (10.880(3) Å), $b = 14.666(2)$ Å (14.733(6) Å), and $c = 21.516(2)$ Å (21.278(7) Å). The metal ions are six-coordinate and the dications are asymmetric (C_1) in the solid state. The MN_6 polyhedra are distorted trigonal prisms. The three five-membered chelate rings M−N−C−C−N of the 1,4,7-triazacyclononane backbone adopt a $(\lambda\lambda\lambda)_5$ (or $(\delta\delta\delta)_5$) conformation whereas two of the six-membered chelate rings of the aniline pendant arms adopt a boat (λ' or δ') and the third adopts a twist-boat conformation (λ'' or δ''). Thus in the solid state the conformation of all three dications is described as $\Lambda(\delta\delta\delta)_5(\lambda''\lambda'\lambda')_6$ and its enantiomeric form as $\Delta(\lambda\lambda\lambda)_5(\delta''\delta'\delta')_6$. In solution, complexes **1**−**3** are fluxional, as shown by a detailed NMR study.

Introduction

It is well established that the tridentate macrocycle 1,4,7-triazacyclononane is ideally suited to bind strongly in a facial fashion in octahedral transition metal complexes. We and others have subsequently shown that N-bound pendant arms with three new functional groups produce hexadentate macrocyclic ligands which form even more kinetically and thermodynamically stable complexes with transition metals in a variety of oxidation states.[2] We have begun to investigate structural and reactivity differences of complexes containing such hexadentate ligands where the pendant arm always is an ortho-substituted benzyl group (Chart 1).[3−9] Thus complexes with three N-bound phenolate or thiophenolate groups have been described. With trivalent transition metal ions such as V(III), Cr(III), Mn(III), Fe(III), and Co(III), extremely stable neutral species LM^{III} were obtained and the effect of π-bonding introduced by the varying donor atoms X has been studied in a systematic fashion.

Chart 1

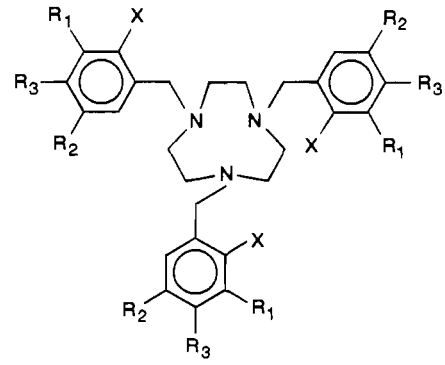

X	R_1	R_2	R_3	Ref.
OH	H	H	H	[4]
OH	CH_3	CH_3	H	[3]
OH	H	$C(CH_3)_3$	H	[7-9]
SH	H	H	$C(CH_3)_3$	[6]
NH_2	H	H	H	this work

[†] Permanent address: Department of Chemistry, University of British Columbia, 2036 Main Mall, Vancouver, British Columbia, Canada V6T 1Z1.

[⊗] Abstract published in *Advance ACS Abstracts,* November 15, 1995.

(1) (a) Max-Planck-Institut für Strahlenchemie. (b) Max-Planck-Institut für Kohlenforschung. (c) Universität Heidelberg.
(2) (a) Chaudhuri, P.; Wieghardt, K. *Prog. Inorg. Chem.* **1987**, *35*, 329. (b) Bhula, R.; Osvath, P.; Weatherburn, D. C. *Coord. Chem. Rev.* **1988**, *91*, 89.
(3) Moore, D. A.; Fanwick, P. E.; Welch, M. J. *Inorg. Chem.* **1989**, *28*, 1504.
(4) Auerbach, U.; Eckert, U.; Wieghardt, K.; Nuber, B.; Weiss, J. *Inorg. Chem.* **1990**, *29*, 938.
(5) Martell, A. E.; Motekaitis, R. J.; Welch, M. J. *J. Chem. Soc., Chem. Commun.* **1990**, 1748.
(6) Beissel, T.; Bürger, K. S.; Voigt, G.; Wieghardt, K.; Butzlaff, C.; Trautwein, A. X. *Inorg. Chem.* **1993**, *32*, 124.
(7) Auerbach, U.; Della Vedova, S. P. C.; Wieghardt, K.; Nuber, B.; Weiss, J. *J. Chem. Soc., Chem. Commun.* **1990**, 1004.
(8) Auerbach, U.; Stockheim, C.; Weyhermüller, T.; Wieghardt, K.; Nuber, B. *Angew. Chem.* **1993**, *105*, 735; *Angew. Chem., Int. Ed. Engl.* **1993**, *32*, 714.
(9) Auerbach, U.; Weyhermüller, T.; Wieghardt, K.; Nuber, B.; Bill, E.; Butzlaff, C.; Trautwein, A. X. *Inorg. Chem.* **1993**, *32*, 508.

0020-1669/95/1334-6440$09.00/0

Table 1. ^{1}H NMR Data for the Ligand L and Complexes **1**–**3**

	proton[g]							
compd	1	2	4	5	7	8	9	10
L[a]	←6.5–7.2 (m)→				2.6	2.6	3.5	4.5
1[b]	7.10	7.24	7.28	7.45	2.60 (7B/8B)	2.95 (7A/8A)	4.09	5.0
1[c]	7.50	7.26	7.50	7.50	2.41 (7A)	3.16 (8A)	4.26 (9A)	6.55 (10A)
					1.56 (7B)	2.65 (8B)	3.81 (9B)	6.04 (10B)
2[d]	←7.35, 7.15, 7.10→				2.70 (7B/8B)	2.95 (7A/8A)	4.04	5.08
2[e]	←6.8–7.5→				←1.7–3.3→		4.65 (9′A)	5.40 (10′A)
							3.90 (9′B)	5.40 (10′B)
							4.45 (9″A)	5.21 (10″A)
							3.65 (9″B)	5.04 (10″B)
							4.01 (9‴A)	4.86 (10‴A)
							3.41 (9‴B)	4.79 (10‴B)
3[f]	7.21	7.06	7.35	7.18	2.67 (7B/8B)	2.95 (7A/8A)	4.15	5.4

[a] Conditions: uncoordinated ligand at T = 300 K, $CDCl_3$, 80 MHz. Atom labeling is the same as that for the coordinated ligand (Chart 2). [b] Conditions: T = 363 K, nitromethane-d_3, 400 MHz. Assignment supported by 2D H,H COSY and 1D NOE experiments. $J(1,2)$ = 1.0 Hz, $J(1,4)$ = 7.8 Hz, $J(2,4)$ = 7.3 Hz, $J(2,5)$ = 7.6 Hz, $J(4,5)$ = 1.7 Hz. NOE enhancement observed by irradiation of protons 9 at protons 5, 7B/8B, 10 and by irradiation of protons 10 at protons 1 and 9. [c] Conditions: T = 193 K, acetone-d_6, 400 MHz. $J(7A,7B)$ = −12.5 Hz, $J(7A,8A)$ = 4.1 Hz, $J(7B,8A)$ = 13.5 Hz, $J(7B,8B)$ = 5.3 Hz, $J(8A,8B)$ = −16.0 Hz, $J(9A,9B)$ = −12.3 Hz. [d] Conditions: T = 363 K, nitromethane-d_3, 400 MHz. Chemical shifts (without assignment) of the different multiplets for aromatic protons are given only. [e] Conditions: T = 273 K, nitromethane-d_3 400 MHz. The primed indices for proton atoms, e.g. 9′A, 9″A, and 9‴A, indicate atoms in the different six-membered chelate rings irrespective of the actual ring conformation. Stereochemical assignment of amine protons 10 as equatorial or axial is *not* made. In contrast, this assignment for the benzylic protons 9 was possible due to observed NOE enhancement of aromatic protons 5 upon irradiation of proton 9B: $J(9'A,9'B)$ = −13 Hz, $J(9''A,9''B)$ = −13 Hz, $J(9'''A,9'''B)$ = −13 Hz, $J(10''A,10''B)$ = −10 Hz, $J(10'''A,10'''B)$ = −10 Hz. Assignment supported by 2D H,H COSY and 1D NOE experiments. [f] Conditions: T = 363 K, nitromethane-d_3, 400 MHz. $J(1,4)$ = 7.8 Hz, J (2,4) = 7.3 Hz, $J(2,5)$ = 7.1 Hz, $J(Hg,9)$ = 58 Hz, $J(Hg,10)$ = 45 Hz. [g] Protons are labeled as in Chart 1.

Here we report the synthesis of such a neutral ligand containing three aniline pendant arms, namely 1,4,7-tris(*o*-aminobenzyl)-1,4,7-triazacyclononane. The coordination chemistry of the ligand aniline as a monodentate ligand is poorly developed.[10] Comparison of the coordination chemistry with Sargeson's 1,4,7-tris(aminoethyl)-1,4,7-triazacyclononane[11] should be interesting because it is well-known that the basicity an amine of a primary alkane differs by at least 5 orders of magnitude from that of aromatic amines such as aniline, which are more acidic. Thus it should be possible to study amide versus amine coordination of L in aqueous solution as a function of pH.

All complexes containing these new ligands with three benzyl pendant arms pose interesting stereochemical problems[3] which are the main theme of the present paper. By facial coordination of the 1,4,7-triazacyclononane backbone of such ligands in an octahedral (or trigonal prismatic) species, three five-membered chelate rings are generated which have λ or δ conformation. In addition, coordination of the three pendant arms gives rise to the formation of three six-membered chelate rings which can also adopt different conformations. Third, in such an octahedral complex, the N_6M polyhedron can have either Λ or Δ configuration due to the presence of three didentate, six-membered chelate rings.

Experimental Section

The ligand 1,4,7-triazacyclononane was prepared according to published procedures.[12] All other chemicals were purchased from commercial sources and used as received.

Caution! Although we have not encountered any problems, it is noted that perchlorate salts are potentially explosive and should be handled with care.

Preparation of the Ligand 1,4,7-Tris(*o*-aminobenzyl)-1,4,7-triazacyclononane. 2-Nitrobenzyl Bromide. To a solution of 2-nitrobenzaldehyde (22.7 g; 0.15 mol) in methanol (100 mL) was added in small amounts of $NaBH_4$ (4.26 g; 0.12 mol). (The reaction is quite exothermic, and the mixture should be efficiently cooled.) After the effervescence had ceased, water (5 mL) was added and the solution was heated to reflux for 1 h. To the cooled solution was added ~0.2 M aqueous HCl (500 mL), whereupon 2-nitrobenzyl alcohol precipitated in voluminous colorless flakes, which were collected by filtration and redissolved in diethyl ether. Addition of dry $MgSO_4$, filtration, and removal of the solvent by rotary evaporation produced the alcohol (yield: 18.4 g (80%)).

To a solution of 2-nitrobenzyl alcohol (18.4 g; 0.12 mol) in CCl_4 (100 mL) was added dropwise with vigorous stirring a solution of PBr_3 (21.6 g; 0.08 mol) in CCl_4 (20 mL). After 60 min of continuous stirring at ambient temperature, the solution was extracted three times with water (200 mL each time). The organic phase was then dried by addition of $MgSO_4$, and the solvent was removed by rotary evaporation. 2-Nitrobenzyl bromide was obtained as an orange-brown viscous liquid that crystallized overnight (yield: 16.6 g (64%)).

1,4,7-Tris(*o*-nitrobenzyl)-1,4,7-triazacyclononane. To a solution of 1,4,7-triazacyclononane (3.31 g; 26 mmol) in toluene (80 mL) was added 2-nitrobenzyl bromide (16.6 g; 77 mmol) and KOH (4.74; 84 mmol). The reaction mixture was stirred for 5 h at 60 °C. After cooling of the orange solution and filtration, it was dried with $MgSO_4$. Removal of the solvent produced an orange-red viscous oil (yield: 13.8 g (98%)). 80 MHz ^{1}H NMR ($CDCl_3$): δ = 2.6 (s, 12 H, $-CH_2CH_2-$), 3.8 (s, 6 H, $-CH_2-$), 7.1–7.9 (m, 12 H, aromatic protons).

1,4,7-Tris(*o*-aminobenzyl)-1,4,7-triazacyclononane (L). To a solution of 1,4,7-tris(*o*-nitrobenzyl)-1,4,7-triazacyclononane (13.8 g; 26 mmol) in ethanol (200 mL) was added graphite powder (3.0 g) as catalyst. The solution was purged with argon, and oxygen-free hydrazine hydrate (31.2 g; 0.62 mol) was added. The reaction mixture was heated to reflux for 12 h under an argon atmosphere. After cooling and filtration of the solution, the solvent was removed by rotary evaporation. The residue was dissolved in $CHCl_3$ (150 mL), the solution was dried with $MgSO_4$, and after filtration the solvent was removed by evaporation. A deep brown resin was obtained that crystallized within a few weeks in the vessel (yield: 10.4 g (90%)). Anal. Calcd for $C_{27}H_{36}N_6$: C, 72.9; H, 8.2; N, 18.9. Found: C, 73.1; H, 8.5; N, 19.0. Solution ^{1}H and ^{13}C NMR data are summarized in Tables 1 and 2. IR (KBr): $\nu_{as}(NH_2)$ 3413, $\nu_s(NH_2)$ 3318 cm^{-1}. Mass spectrum: molecular ion peak at *m/z* 444 (calcd 444.6).

[LH]ClO_4. Addition of a few drops of 2 M $HClO_4$ to a solution of L in ethanol initiated the precipitation of yellow crystals of the

(10) House, D. A. In *Comprehensive Coordination Chemistry*; Wilkinson, G., Gillard, R. D., McCleverty, J. A., Eds.; Pergamon Press: Oxford, England, 1987; Vol. 2, p 59.
(11) (a) Gahan, L.; Lawrance, G. A.; Sargeson, A. M. *Aust. J. Chem.* **1982**, *35*, 1119. (b) Hammershoi, A.; Sargeson, A. M. *Inorg. Chem.* **1983**, *22*, 3554.
(12) Wieghardt, K.; Schmidt, W.; Nuber, B.; Weiss, J. *Chem. Ber.* **1979**, *112*, 2220.

Table 2. 100.6 MHz ^{13}C NMR Data for the Uncoordinated Ligand L and Complexes **1**−**3** in Solution at $T = 300$ K (L, **3**) and at $T = 363$ K (**1**, **2**)[a]

	position[b]								
compd	1	2	3	4	5	6	7	8	9
L	115.5 d	117.1 d	123.3 s	128.7 d	131.1 d	148.3 s	56.4 t	56.4 t	62.8 t[c]
1	122.9	127.1	127.5	132.3	133.7	142.2	54.1	54.1	62.9[d]
2	122.7	126.4	126.9	132.3	133.9	142.2	53.7	53.7	62.5
3	122.6	126.0	*e*	132.3	134.3	143.3	53.6	53.6	*f*

[a] Solvents: acetone-d_6 for L; nitromethane-d_3 for **1** and **2**; acetonitrile-d_3 for **3**. [b] For atom labels see Chart 2. [c] The same C,H-multiplicity pattern holds for complexes **1**−**3**. [d] Assignment supported by 2D H,C COSY spectroscopy. [e] Due to poor solubility of **3**, not found. [f] Hidden by solvent signal.

Table 3. Crystallographic Data for Complexes **1**−**3**

	1	**2**	**3**
empirical formula	$C_{27}H_{36}N_6Cl_2O_8Zn$	$C_{27}H_{37}N_6Cl_2O_{8.5}Cd$	$C_{27}H_{37}N_6Cl_2O_{8.5}Hg$
fw	708.9	764.9	853.1
space group	$P2_1/n$ (No. 14)	$Pc2_1n$ (nonstd setting of No. 33)	$Pc2_1n$ (nonstd setting of No. 33)
a, Å	9.222(5)	10.882(2)	10.880(3)
b, Å	17.01(1)	14.666(2)	14.733(6)
c, Å	19.41(1)	21.516(2)	21.278(7)
β, deg	97.03(5)		
V, Å^3	3021.9(12)	3433.8(6)	3410.8(8)
Z	4	4	4
ρ(calcd), g cm^{-3}	1.56	1.48	1.66
temp, °C	20	20	22
radiation (λ, Å)	Mo Kα (0.710 73)	Mo Kα (0.710 73)	Mo Kα (0.710 73)
abs coeff, mm^{-1}	1.07	0.84	4.72
min/max transm coeff	0.88/1.00	0.94/1.00	0.53/1.00
R^a	0.045	0.061	0.051
$R_w{}^b$	0.036	0.057	0.046

[a] $R = \Sigma(|F_o| - |F_c|)/\Sigma|F_o|$. [b] $R_w = \{\Sigma w(|F_o| - |F_c|)^2/\Sigma w(|F_o|)^2\}^{1/2}$.

monohydroperchlorate of L. Anal. Calcd for $C_{27}H_{37}N_6ClO_4$: C, 59.4; H, 6.8; N, 15.4; ClO_4, 22.4. Found: C, 59.4; H, 6.8; N, 14.9; ClO_4, 23.0.

Preparation of Complexes. [LZn](ClO$_4$)$_2$ (1). To a solution of the ligand L (0.22 g; 0.5 mmol) in methanol (10 mL) was added a solution of $Zn(ClO_4)_2 \cdot 6H_2O$ (0.19 g; 0.5 mmol) in ethanol (10 mL). In cases where the resulting solution was turbid, two drops of 60% $HClO_4$ were added. The solution was heated to reflux for 30 min. Upon cooling of the mixture to 20 °C, a pale yellow microcrystalline precipitate formed, which was collected by filtration, washed with ethanol and ether, and air-dried. Single crystals suitable for X-ray crystallography were obtained when the above reaction was carried out in twice the amount of solvent. Yield: 0.25 g (71%). Anal. Calcd for $C_{27}H_{36}N_6Cl_2O_8Zn$: C, 45.7; H, 5.1; N, 11.9; ClO_4, 28.1. Found: C, 45.5; H, 5.2; N, 11.8; ClO_4, 28.5. UV−vis (CH_3CN): $\lambda_{max} = 225$ nm ($\epsilon = 12.9 \times 10^3$ L mol^{-1} cm^{-1}), 276 (1.5×10^3), 294 (1.1×10^3). Solution ^1H, ^{13}C NMR: Tables 1 and 2.

[LCd](ClO$_4$)$_2$·0.5H$_2$O (2). The pale yellow complex was prepared as described for **1** by using $Cd(ClO_4)_2 \cdot 6H_2O$ (0.21 g; 0.5 mmol). Yield: 0.26 g (68%). Anal. Calcd for $C_{27}H_{36}N_6Cl_2O_8Cd \cdot 0.5H_2O$: C, 42.4; H, 4.9; N, 11.0. Found: C, 42.4; H, 5.0; N, 10.8. UV−vis (CH_3CN): $\lambda_{max} = 231$ nm ($\epsilon = 12.9 \times 10^3$ L mol^{-1} cm^{-1}), 270 (2.4×10^3). Solution ^1H, ^{13}C NMR: Tables 1 and 2. ^{113}Cd CP/MAS NMR, $T = 297$ K: $\delta = 247$, anisotropy region 380−90 ppm, $W^{1/2} = 530$ Hz.

[LHg](ClO$_4$)$_2$·0.5H$_2$O (3). The pale yellow complex was prepared as described for **1** by using $Hg(ClO_4)_2 \cdot 6H_2O$ (0.5 mmol). Yield: 0.25 g (60%). Anal. Calcd for $C_{27}H_{36}N_6Cl_2O_8Hg \cdot 0.5H_2O$: C, 38.4; H, 4.3, N, 10.0. Found: C, 38.7; H, 4.4; N, 10.3. UV−vis (CH_3CN): $\lambda_{max} = 231$ nm ($\epsilon = 12.7 \times 10^3$ L mol^{-1} cm^{-1}), 274 (2.5×10^3). Solution ^1H, ^{13}C NMR: Tables 1 and 2. Single crystals suitable for X-ray crystallography were obtained by recrystallization from acetonitrile solution.

X-ray Structure Determinations. Intensities and lattice parameters of a pale yellow, translucent, irregularly shaped crystal of **1**, a pale yellow needle-shaped crystal of **2**, and a colorless platelet of **3** were measured on a Syntex R3 diffractometer at ambient temperature by using monochromated Mo Kα radiation. Crystal parameters and details of the data collection and refinement are summarized in Table 3 (for full details see the Supporting Information). Complexes **2** and **3** crystallize in the orthorhombic space group $Pna2_1$ (No. 33) and were refined in the nonstandard setting $Pc2_1n$; **1** was refined in the nonstandard setting $P2_1/n$ of space group No. 14. Empirical absorption corrections were carried out in each case. The structures were solved by conventional Patterson and Fourier methods. The Siemens program package SHELXTL-PLUS was used.[13] The function minimized during full-matrix least-squares refinement was $\Sigma w(|F_o| - |F_c|)^2$, where $w^{-1} = \sigma^2(F)$. Neutral-atom scattering factors and anomalous-dispersion corrections for non-hydrogen atoms were taken from ref 14. The hydrogen atoms were placed at calculated positions with isotropic thermal parameters. Crystals of **2** were of poor X-ray quality and, consequently, the accessible 2θ range was rather small (<46°). The numerical stability of the solution suffered somewhat, and the thermal parameters of C15−C20 of one of the aromatic rings are unreasonably large. Tables of atom coordinates for **1**−**3** are available in the Supporting Information.

Physical Measurements. Solution NMR spectra were recorded on Bruker WP 80 (^1H), AMX (^{13}C), and AM 400 (^1H, ^{13}C) spectrometers. ^1H and ^{13}C NMR signals are referenced to external TMS. Solid state CP/MAS ^{13}C and ^{113}Cd NMR spectra were measured on a Bruker MSL-300 spectrometer equipped with CP/MAS double-bearing probe and a Bruker BV-1000 temperature control unit. ZrO_2 rotors (7 mm o.d.) completely or partially filled (under argon) were spun at spin rates of 4 kHz. External standards: adamantane for ^{13}C CP/MAS spectra, δ_{TMS} (CH_2) 38.40; $CdSO_4 \cdot 8H_2O$ for ^{113}Cd CP/MAS spectra, δ(solid Cd-$(ClO_4)_2$) = −61.0 and −48.0.[15] Typical 90° pulses: ca. 4 s for ^1H; 4.3 s for ^{113}Cd. Infrared spectra were recorded in the 4000−400 cm^{-1} range as KBr disks on a Perkin-Elmer FT IR 1720X spectrometer. UV−vis spectra were measured on a Perkin-Elmer Lambda 9 spectrophotometer in the range 200−1000 nm.

(13) Full-matrix least-squares structure refinement program package SHELXTL-PLUS: G. M. Sheldrick, Universität Göttingen.
(14) *International Tables for Crystallography*; Kynoch: Birmingham, England, 1974; Vol. IV, pp 99, 149.
(15) Honken, R. S.; Doty, F. D.; Ellis, P. D. *J. Am. Chem. Soc.* **1983**, *105*, 4163.

Results and Discussion

Synthesis. The synthetic route to the ligand 1,4,7-tris(*o*-aminobenzyl)-1,4,7-triazacyclononane (L) is briefly described as follows. Key steps involve N-binding of 2-nitrobenzyl bromide to 1,4,7-triazacyclononane in toluene over KOH. Subsequently, the NO_2 groups of 1,4,7-tris(*o*-nitrobenzyl)-1,4,7-triazacyclononane are reduced to $-NH_2$ groups by hydrazine hydrate by using graphite as catalyst.[16] The electronic spectrum of L in CH_3CN displays two absorption maxima at 246 nm ($\epsilon = 16.6 \times 10^3$ L mol^{-1} cm^{-1}) and 291 nm (ϵ 5.2 $\times 10^3$) which are assigned to $\pi \rightarrow \pi^*$ transitions of the aromatic amine functionality (p- and α-bands). Addition of perchloric acid to an ethanolic solution of L produces yellow crystals of [LH]-(ClO_4).

The complexes $[LZn](ClO_4)_2$, **1**, $[LCd](ClO_4)_2 \cdot 0.5H_2O$, **2**, and $[LHg](ClO_4)_2 \cdot 0.5H_2O$, **3**, were prepared by the reaction of the respective metal ion perchlorate salt $M(ClO_4)_2 \cdot 6H_2O$ and the ligand L (1:1) in ethanol. Yellow to colorless crystals of **1** and pale yellow crystals of **2** and **3** were obtained in satisfactory yields (>60%). In the infrared spectra of **1**−**3** (KBr disks) the coordinated amine groups display the $\nu_{as}(NH_2)$ and $\nu_s(NH_2)$ stretching frequencies at 3337/3317 and 3260/3240 cm^{-1} for **1**, 3317 and 3262 for **2**, and 3320 and 3256 cm^{-1} for **3**. The $\delta(NH_2)$ modes are observed at 1584 cm^{-1} (**1**), 1585 cm^{-1} (**2**), and 1588 cm^{-1} (**3**).

Crystal Structures. Crystals of **1**−**3** consist of the dications $[LZn]^{2+}$, $[LCd]^{2+}$, and $[LHg]^{2+}$, respectively, and well-separated perchlorate anions. Complexes **2** and **3** crystallize as hemihydrates whereas **1** does not contain water molecules of crystallization. Note that **1** crystallizes in the monoclinic space group $P2_1/n$, whereas **2** and **3** are isostructural and crystallize in the orthorhombic space group $Pna2_1$ with very similar unit cell dimensions. Figure 1 displays perspective views of the structures of the dications in crystals of **1**−**3** and gives the corresponding atom-labeling schemes. Table 4 summarizes important bond distances and angles.

The hexadentate neutral ligand 1,4,7-tris(*o*-aminobenzyl)-1,4,7-triazacyclononane provides six N-donor atoms which are coordinated to the metal ion Zn^{2+} in **1**, Cd^{2+} in **2**, and Hg^{2+} in **3**. The resulting N_6M polyhedron is best described as distorted trigonal prismatic. The twist angle ϑ defined as

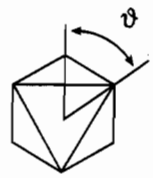

is 13.6° in **1** and 18° in **2** and **3**. The angle ϑ is 0° in a regular trigonal prism and 60° in an octahedron.

The average Zn−N bond length is 2.23 Å, which compares well with those of other ZnN_6 polyhedra reported in the literature.[17] The same holds for the average Cd−N distance of 2.37 Å[18] and the average Hg−N bond length of 2.43 Å.[19] In the present cases, there is no significant difference between the metal−nitrogen bond distances of the tertiary amine nitrogen donors, on the one hand, and the aniline nitrogen donors, on the other hand.

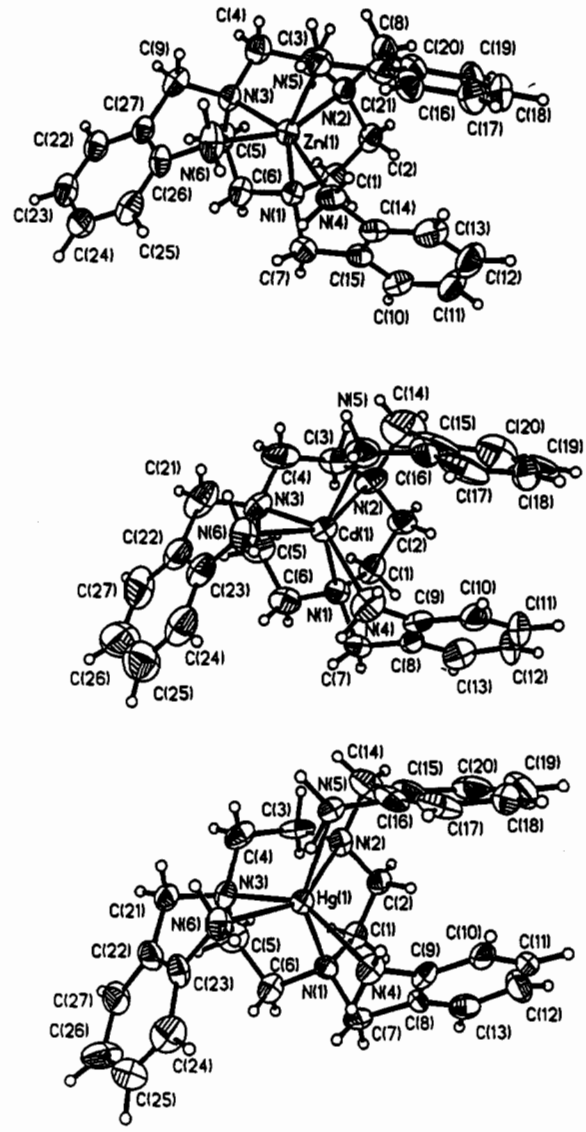

Figure 1. Structure of the dications in crystals of **1** (top), **2** (middle), and **3** (bottom).

The coordinated 1,4,7-triacyclononane backbone of the ligand L forms three five-membered chelate rings M−N−C−C−N which adopt a $(\lambda\lambda\lambda)_5$ or $(\delta\delta\delta)_5$ conformation. This has been observed for all complexes containing this facially bound cyclic triamine moiety. In no instance has "conformational mix" like $(\lambda\delta\delta)/(\delta\lambda\lambda)$ or $(\lambda\lambda\delta)/(\delta\delta\lambda)$ has been observed. These mixed forms are more strained than the $(\lambda\lambda\lambda)_5$ or $(\delta\delta\delta)_5$ form and are, therefore, energetically unfavorable.

The three coordinated pendant aniline arms form three six-membered chelate rings of the type $M-N_{amine}-CH_2-C{=}C-N_{aniline}$ in complexes **1**−**3**. In the solid state, structures of the dications two of these six-membered chelate rings have a boat conformation whereas the third adopts a twist-boat

(16) Han, B. H.; Shin, D. H.; Cho, S. Y. *Tetrahedron Lett.* **1985**, *26*, 6233.
(17) Typical Zn−N distances in N_6Zn complexes: 2.17(1) Å in $[(tacn)_2Zn]^{2+}$ (tacn = 1,4,7-triazacyclononane) [Chaudhuri, P.; Stockheim, C.; Wieghardt, K.; Deck, W.; Gregorzik, R.; Vahrenkamp, H.; Nuber, B.; Weiss, J. *Inorg. Chem.* **1992**, *31*, 1451]; 2.213(4) Å in $[ZnL'_2]^{2+}$ (L' = tris((methylamino)methyl)ethane) [Brandt, W.; Wirbser, J.; Powell, A. K.; Vahrenkamp, H. *Z. Naturforsch.* **1991**, *46B*, 440].
(18) Typical Cd−N distances in N_6Cd complexes: 2.36(1) Å in $[(tacn)_2Cd]^{2+}$ (tacn = 1,4,7-triazacyclononane) [Strasdeit, H.; Dahme, A. K.; Weber, M.; Pohl, S. *Acta Crystallogr.* **1992**, *C48*, 437]; 2.38 Å in $[Cd(en)_3]^{3+}$ (en = ethylenediamine) [Mahadevan, C.; Seshasayee, M.; Sastry, S.; Subrahmanyan, C. *Z. Kristallogr.* **1985**, *171*, 173]; 2.410−2.423 Å in $[CdL^2](ClO_4)_2$ (L^2 = 6,13-dimethyl-1,4,8,11-tetraazacyclotradecane-6,13-diamine) [Bernhard, P. V.; Comba, P.; Hambley, T. W.; Lawrance, G. A.; Várnagy, K. *J. Chem. Soc., Dalton Trans.* **1992**, 355].
(19) In $[Hg(en)_2](ClO_4)_2$ an average Hg−N distance of 2.32 Å has been reported: Duplanicic, T. J. *J. Chem. Soc., Dalton Trans.* **1976**, 887.

Table 4. Selected Distances (Å) and Angles (deg) of Complexes **1**–**3**

		Complex **1**			
Zn1–N1	2.205(4)	N4–C14	1.446(7)	N3–Zn1–N6	84.0(2)
Zn1–N2	2.235(4)	N5–C21	1.458(7)	N4–Zn1–N6	87.4(2)
Zn1–N3	2.248(5)	N6–C26	1.444(7)	N5–Zn1–N6	87.3(1)
Zn1–N4	2.246(4)	N1–Zn1–N2	80.8(2)	Zn1–N1–C1	109.6(3)
Zn1–N5	2.275(4)	N1–Zn1–N3	80.4(2)	Zn1–N1–C6	104.0(3)
Zn1–N6	2.181(4)	N2–Zn1–N3	80.6(2)	Zn1–N1–C7	112.8(3)
N2–Zn1–N4	112.3(2)	N1–Zn1–N4	85.8(2)	Zn1–N4–C14	117.1(3)
N3–Zn1–N4	159.4(2)	N1–Zn1–N5	157.6(1)	Zn1–N5–C21	108.5(3)
N2–Zn1–N5	83.2(2)	N3–Zn1–N5	112.5(2)	Zn1–N6–C26	120.5(3)
N4–Zn1–N5	85.7(1)	N1–Zn1–N6	113.0(2)		
N2–Zn1–N6	157.3(2)				
		Complex **2**			
Cd1–N1	2.38(1)	N4–C9	1.43(2)	N2–Cd1–N5	81.0(5)
Cd1–N2	2.39(1)	N5–C16	1.44(3)	N4–Cd1–N6	87.9(5)
Cd1–N3	2.36(2)	N6–C23	1.41(2)	N5–Cd1–N6	88.6(5)
Cd1–N4	2.36(1)	N1–Cd1–N2	75.6(5)	Cd1–N1–C1	111.1(10)
Cd1–N5	2.37(2)	N1–Cd1–N3	76.5(5)	Cd1–N1–C6	104.0(11)
Cd1–N6	2.35(1)	N2–Cd1–N3	76.0(5)	Cd1–N1–C7	113.0(10)
N3–Cd1–N5	117.2(5)	N1–Cd1–N4	82.2(5)	Cd1–N4–C9	109.9(10)
N4–Cd1–N5	94.1(5)	N2–Cd1–N4	123.0(5)	Cd1–N5–C16	109.1(12)
N1–Cd1–N6	121.8(5)	N3–Cd1–N4	146.7(5)	Cd1–N6–C23	112.1(11)
N2–Cd1–N6	147.8(5)	N1–Cd1–N5	149.0(5)		
N3–Cd1–N6	82.1(5)				
		Complex **3**			
Hg1–N1	2.45(1)	N4–C9	1.43(2)	N5–Hg1–N6	89.9(5)
Hg1–N2	2.46(1)	N5–C16	1.35(3)	N2–Hg1–N6	148.5(5)
Hg1–N3	2.41(1)	N6–C23	1.46(2)	N4–Hg1–N6	90.1(5)
Hg1–N4	2.41(1)	N1–Hg1–N2	74.3(5)	Hg1–N1–C1	110.6(10)
Hg1–N5	2.43(1)	N2–Hg1–N3	76.1(5)	Hg1–N1–C6	102.1(10)
Hg1–N6	2.40(1)	N2–Hg1–N4	120.0(4)	Hg1–N1–C7	109.9(10)
N1–Hg1–N3	74.7(5)	N1–Hg1–N5	147.8(5)	Hg1–N4–C9	109.9(9)
N1–Hg1–N4	83.2(5)	N3–Hg1–N5	118.9(5)	Hg1–N5–C16	108.9(13)
N3–Hg1–N4	148.0(5)	N1–Hg1–N6	121.8(5)	Hg1–N6–C23	111.0(10)
N2–Hg1–N5	80.9(5)	N3–Hg1–N6	82.5(5)		
N4–Hg1–N5	92.0(5)				

conformation. This is schematically shown in Figure 2. In the following, we will use the notations λ' and δ' for the two enantiomeric forms of the boat conformation and λ''/δ'' for the twist-boat conformations of these six membered chelate rings. A third source of chirality has to be considered. Since the MN_6 polyhedra are not exactly trigonal prismatic, the presence of three pendant arm chelate rings allows enantiomeric Λ and Δ configurations of the MN_6 polyhedron.

Inspection of the crystal structure data reveals that in **1**–**3** both enantiomers $\Lambda(\lambda\lambda\lambda)_5(\delta''\delta'\delta')_6$ and $\Delta(\delta\delta\delta)_5(\lambda''\lambda'\lambda')_6$ co-crystallize in equal amounts (racemate).

It is important to recognize at this point that although the dications in **1**–**3** have no crystallographic symmetry (C_1), they adopt the same overall structure with identical conformations of the three five-membered chelate rings but two different conformations of the six-membered pendant arm rings. This is somewhat surprising because the increasing ionic radii of the central metal ion (Zn^{2+} 0.88 Å, Cd^{2+} 1.09 Å, and Hg^{2+} 1.16 Å) with coordination number 6 and invariant C–C, C–N distances within the ligand could be expected to induce conformational changes which are not observed. Furthermore, since **1** and **2**, **3** crystallize in different space groups, this effect cannot be rationalized by packing effects in the solid state. In fact, neither the perchlorate anions nor the water molecules of crystallization are involved in any significant O···H–N hydrogen bonding contacts with the amine protons of the aniline pendant arms. Intramolecular interactions between the NH_2 groups are also not present nor are there intermolecular stacking effects of the phenyl rings.

If in the asymmetric dication, the one six-membered chelate ring with twist-boat conformation undergoes an intramolecular conversion to the boat conformation ($\lambda'' \rightarrow \lambda'$ or $\delta'' \rightarrow \delta'$) the resulting cation possesses C_3 symmetry $\Lambda(\delta\delta\delta)_5(\lambda'\lambda'\lambda')_6$ or $\Delta(\lambda\lambda\lambda)_5(\delta'\delta'\delta')_6$. As we will show in a subsequent paper, this structure is adopted in the solid state by the octahedral nickel(II) complex $[LNi](ClO_4)_2$.[20]

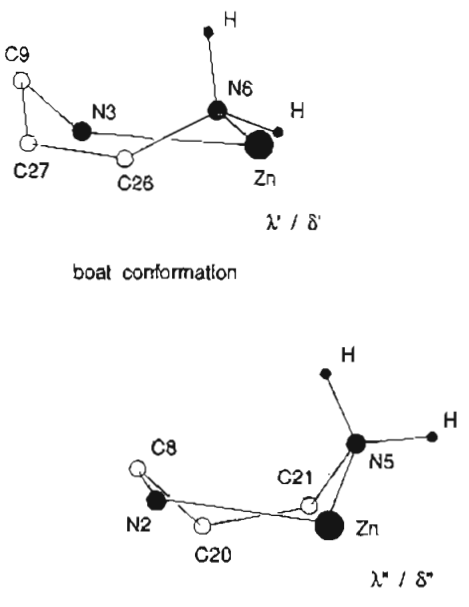

Figure 2. Schematic representation of the two observed conformations of the three six-membered pendant arm chelate rings in the dications of **1**–**3**.

(20) Schlager, O.; Wieghardt, K.; Nuber, B. *Inorg. Chem.*, **1995**, *34*, 6449.

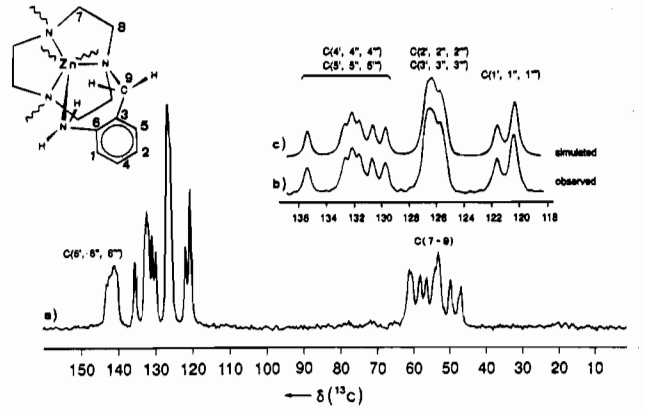

Figure 3. 75.4 MHz ^{13}C CP/MAS NMR spectra of **1** (a). The inset (b) shows an expansion of the region $\delta = 118-136$ of aromatic carbon atoms C1–C5 and trace c a deconvolution with Lorentz lines. The primed indices for C atoms, e.g. C′, C″, and C‴, indicate a given atom within different six-membered rings irrespective of their actual conformation.

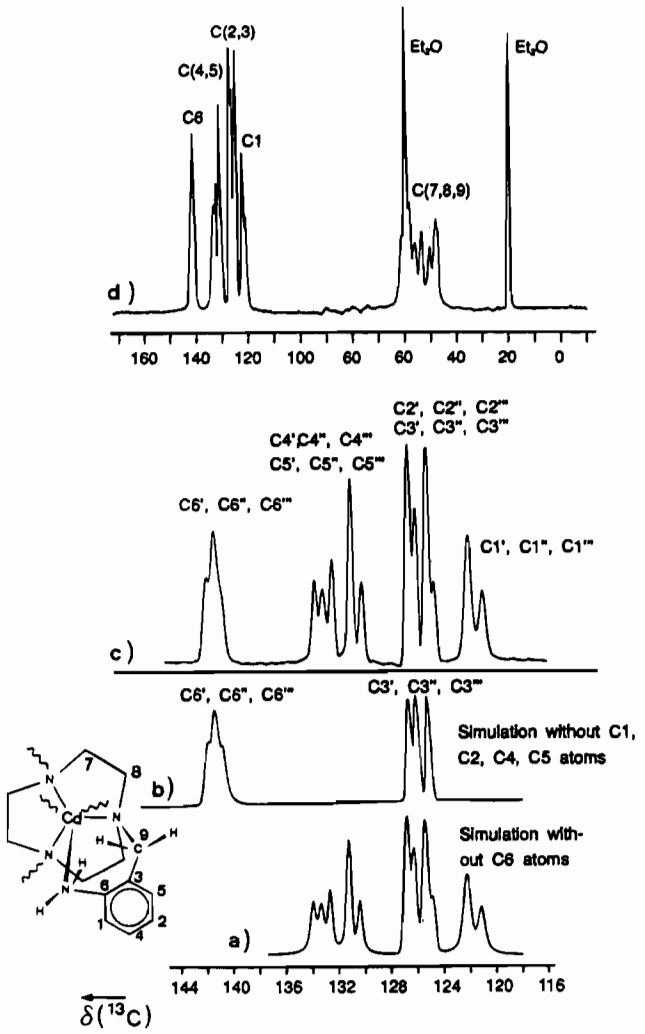

Figure 4. 75.4 MHz ^{13}C CP/MAS NMR spectrum of **2** (d), expansion of the aromatic region (c), and deconvoluted spectra of the aromatic carbon atoms C1–C6 (a, b). Crystals of **2** were washed with diethyl ether which is detected as an impurity.

Solid State NMR Spectra of Complexes 1 and 2. Solid state CP/MAS ^{13}C NMR spectra of **1** and **2** are displayed in Figures 3 and 4, respectively. The labeling scheme shown in Chart 2 for carbon and hydrogen atoms is used throughout. We will use primed indices for the carbon atoms, e.g. C1′, C1″, or C1‴, to indicate a given atom in the first, second, or third six-membered chelate ring regardless of its actual conformation. Since the dications in **1**–**3** possess C_1 symmetry, all three six-membered chelate rings are chemically inequivalent and each carbon atom is expected to show a resonance at a different value of the chemical shift δ. Thus a total of 27 resonances (18 aromatic C atoms, 3 benzylic C atoms, and 6 ethylene C atoms) are, in principle, observable. On the other hand, for a C_3-symmetric dication, only 9 such signals are expected. Figures 3 and 4 clearly show that more than 9 signals are detectable in the solid state. The aromatic carbon resonances of solid **1** and **2** are observed in the region $\delta = 110-150$ whereas the benzyl and ethylene carbon atoms resonate in the region $\delta = 40-70$.

Chart 2

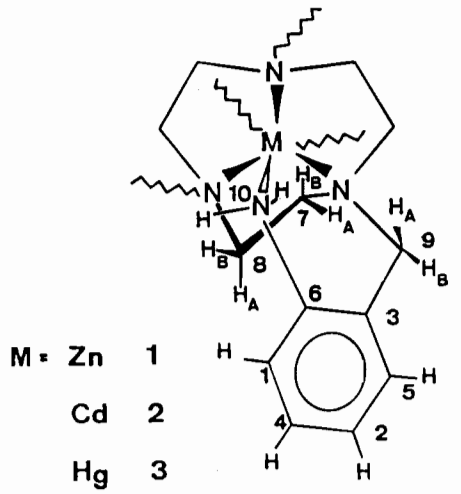

The differences in chemical shift δ are not sufficiently large to fully resolve all expected 27 resonances. Nevertheless, it is possible to obtain definitive evidence for C_1 symmetry of complexes **1** and **2** in the solid state. NQS (nonquaternary suppression) spectra revealed two groups of lines for quaternary carbon atoms at $\delta \sim 140$ and ~ 126 ppm for both **1** and **2**, respectively. The first group corresponds to signals of the C6 atoms and is not resolved. It is noted that these signals may be broadened or even split due to quadrupole interactions with the adjacent ^{14}N atoms.[21] The second group of signals at ~ 126 ppm displays three well-resolved lines of equal intensity (1:1:1) for the C3 atoms of **2** (Figure 4, trace b) and two signals at 126.3 and 125.4 ppm (intensity ratio 2:1) in the spectrum of **1** (not shown). The splitting patterns of the signals of the protonated aromatic carbon atoms (C1, C4, C2, and C5) in the region $\delta = 136-118$ for **1** and **2** are indicative of and fully consistent with the presence of three chemically inequivalent disubstituted aromatic rings, respectively. Furthermore, nearly all of the nine aliphatic carbon atoms show a resolved signal in the region 45–65 ppm: 8 resonances for complex **1** (Figure 3, trace a)) and 7 for complex **2** (Figure 4, trace d)) are observed.

A Lorentz fit of the aromatic parts of the ^{13}C CP/MAS spectrum for **1** is shown in Figure 3 (trace c) and for **2** in Figure 4 (trace a). In a series of deconvolution calculations, a good fit to the experimental spectrum was obtained with 15 signals of nearly equal intensity (4–5% root-mean-square error).

In the ^{113}Cd CP/MAS spectrum of solid **2**, we have detected only one signal at $\delta = 224$ ppm with a line half-width of 530 Hz which is independent of the temperature (303–200 K) and other experimental conditions. The observed chemical shift agrees well with other six-coordinate amine complexes of Cd^{2+}.[22] This clearly shows that in crystals of **2** only one

(21) Harris, R. K.; Olivieri, A. C. *Prog. NMR Spectrosc.* **1992**, *24*, 435.
(22) Munakata, M.; Kitagawa, S.; Yagi, F. *Inorg. Chem.* **1986**, *25*, 964.

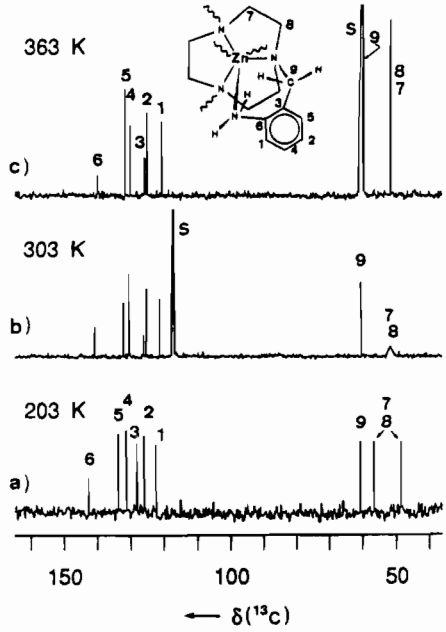

Figure 5. Variable-temperature 100.6 MHz ^{13}C NMR spectra of **1** in solution: (a) solent acetone-d_6, T = 203 K; (b) solvent acetonitrile-d_3, T = 303 K; (c) solvent nitromethane-d_3, T = 363 K. "S" denotes solvent signals.

diastereoisomer is present, in agreement with the crystal structure determination.

Thus, the solid state NMR spectra of **1** and **2** are in excellent agreement with the crystallography determined asymmetric structures of the dications in **1** and **2**.

Dynamic Behavior of Complexes 1−3 in Solution. The solution behavior of **1−3** has been investigated by temperature-dependent ^1H and ^{13}C NMR spectroscopy. Figure 5 shows variable-temperature ^{13}C NMR solution spectra of freshly prepared samples of **1**. They are of striking simplicity as compared to the corresponding solid state spectrum. At 203 K (trace a), only six resonances of aromatic C atoms (C1−C6) at δ = 115−150 and three signals for aliphatic carbon atoms (C7−C9) at δ = 45−65 are observed. Signals for the ethylene carbon atoms of the 1,4,7-triazacyclononane backbone C7 and C8 at δ = 48.5 and 56.7 coalesce, and upon increases in the temperature to 303 K (trace b) and to 363 K (trace c), only one signal at δ = 54 is observed; the number of signals of aromatic and benzylic C atoms remains unaffected (Table 2). Considerably more complex ^{13}C NMR spectra of samples have been observed in acetone-d_6 (containing traces of H_2O/D_2O) when the samples were allowed to stand at room temperature in a sealed NMR tube for a few hours. Some resonances broaden and others even split. These effects are time and temperature dependent and point to the slow formation of *H/D* isotopomers of complexes in acetone-d_6 containing small amounts of H_2O. Parallel to these spectral changes, a decrease in the intensity of signals for the protons of the NH_2 groups (10A and 10B) in the ^1H NMR spectrum is observed (see below). It is noted that up to six NH_2 protons are exchangeable in each dication. In the ^1H NMR spectrum of **1** in acetone-d_6 at 243 K (Figure 6, trace a), this H/D exchange is clearly revealed by the following observations: (i) The intensity of the ^1H signals of the NH_2 groups (10A and 10B) is decreased relative to those of other proton resonances after a short time and (ii) these signals show no vicinal H,H coupling constant.

Consequently, in acetone solution these *inter*molecular exchange processes superimpose spectral changes on those due to the *intra*molecular molecular dynamics of the dications and

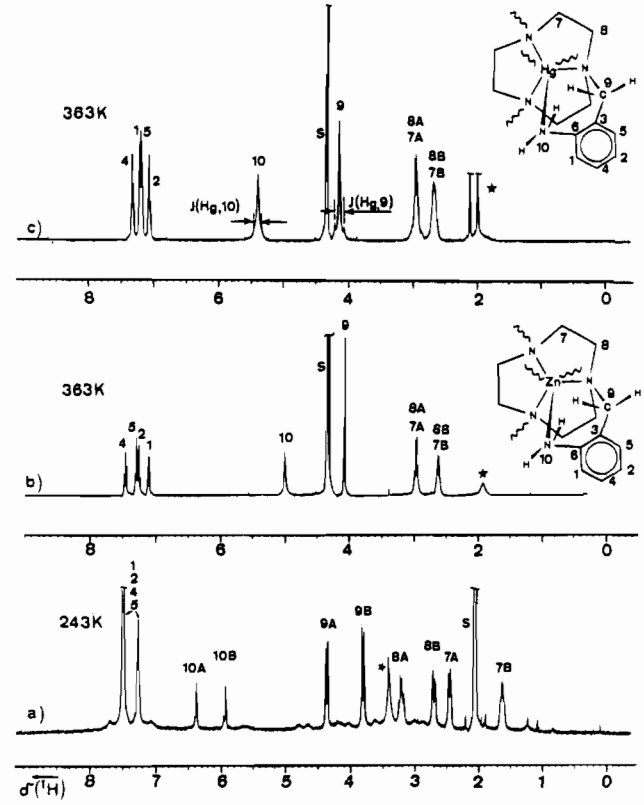

Figure 6. Variable-temperature 400 MHz ^1H NMR spectra of **1** (a, b) and **3** (c) in solution: (a) solvent acetone-d_6, T = 243 K (for atom labeling see Chart 2); (b, c) solvent nitromethane-d_3, T = 363 K. "S" denotes solvent signals; asterisks denote H_2O and/or other impurities.

definitive conclusions regarding the latter process from acetone solution spectra are difficult. Despite these problems, we include these spectra in the following because it has been important to decrease the temperature to −80 °C, where nitromethane and acetonitrile are already frozen.

In spite of these limitations, some temperature-dependent spectral changes can be analyzed and interpreted. At 243 K, the signals of the benzylic protons 9A at 4.26 ppm and 9B at 3.81 ppm appear as doublets with a coupling constant of −12.3 Hz. Analysis of the {AMXZ} spin system of the 1,4,7-triazacyclononane backbone (ethylene protons 7 and 8) as shown in Table 1 and Chart 2 indicates that the three five-membered M−N−C−C−N chelate rings adopt a single preferred conformation ($\lambda\lambda\lambda$ or $\delta\delta\delta$) at this low temperature. Upon warming of the solution, the stereochemical differentiation of both the benzylic and the ethylene protons disappears. At room temperature (not shown), the ^1H NMR spectra display strongly broadened resonances for both benzylic protons 9 and for both aniline protons 10 and two structureless broad signals for the protons 7A, 8A and 7B, 8B. Further heating to 363 K (Figure 6, trace b) results in a decrease of the line width, and consequently, the signal of protons 9 (=9A + 9B) appears as a sharp singlet at an average δ of 4.10 ppm. The still existing broadening of the signal of protons 10 (=10A + 10B) and the observed small shift of its chemical shift ($\delta(10) \neq {}^1/_2[\delta(10A) + \delta(10B)]$) are due to the presence of different H/D isotopomers as discussed above. The observation of sharp resonances makes stereochemical assignments shown in Chart 2 and Figure 6 for complex **1** at 363 K possible. This has been achieved by an analysis of the coupling constants and a series of 2D H,H COSY and 1D NOE experiments (Table 1).

An important question pertains to the actual denticity of the ligand L in complexes **1−3** at elevated temperatures in solution.

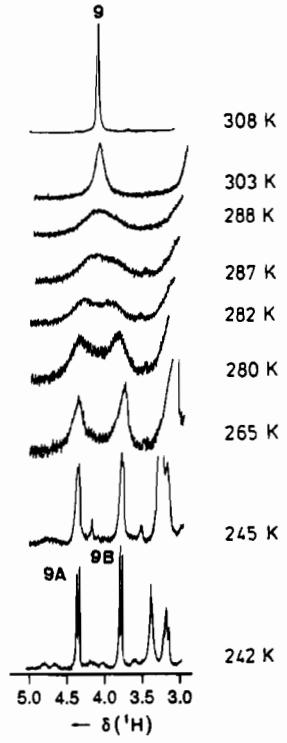

Figure 7. Variable-temperature 400 MHz ^{1}H NMR spectra of the benzylic protons 9A and 9B of **1** in acetone-d_6 (for atom labeling see Chart 2).

It is therefore gratifying that the nitromethane-d_3 solution ^{1}H NMR spectrum of **3** at 363 K (Figure 6, trace c), which is very similar to that of **1** using the same conditions (Figure 6, trace b), shows the coupling of the aniline protons 10 and of the benzylic protons 9 with the ^{199}Hg isotope (16.8% abundance), respectively. These scalar couplings prove that even at 363 K all six nitrogen donor atoms are coordinated to the metal ion.

Analysis of the temperature dependence of the line shape (Figure 7) of the diastereotopic proton signals 9A and 9B, which at elevated temperature are equivalent, allowed us to estimate an activation barrier $\Delta G^{\ddagger}$ of 55 ± 1 kJ mol^{-1} for the intramolecular dynamic process of **1**.[23]

The ^{13}C NMR spectrum of **2** in nitromethane-d_3 at 363 K is very similar to that of **1** except for the fact that the ethylene bridge carbon signal C7, C8 is still exchange broadened in contrast to the same signal of **1** at that temperature. This observation indicates that complete freezing of the molecular dynamics of **2** takes place at a higher temperature than that of **1** and that its activation barrier is larger. Indeed, already at 274 K, an increased number of broad ^{13}C signals of the ethylene bridge carbon atoms are discernible which upon further cooling yield sharp resonances (Figure 8, trace a). Concomitantly, the number of aromatic carbon atom signals C1−C6 increases. Regrettably, the signals of the benzylic carbon atoms at 363 and 273 K are hidden under solvent signals and could not be observed.

Low-temperature measurements were again performed in acetone-d_6 solution in which the above discussed *inter*molecular H/D exchange takes place. The ^{13}C NMR spectrum of **2** at 203 K in Figure 8 (traces a, b) represents therefore the sum of these *intra*- and *inter*molecular dynamic effects.

The variable-temperature ^{1}H NMR spectra of **2** dissolved in nitromethane-d_3 (Figure 9) are more readily interpreted. At 283 K, six doublets at ~4 ppm with a vicinal coupling constant

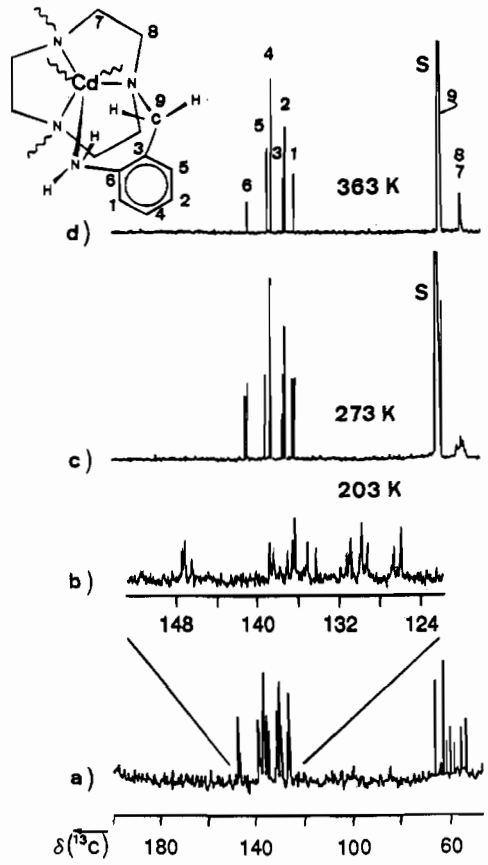

Figure 8. Variable-temperature 100.6 MHz ^{13}C NMR spectra of **2** in solution: (a, b) solvent acetone-d_6, T = 203 K; (c, d) solvent nitromethane-d_3 at T = 273 and 363 K, respectively. "S" denotes solvent signals.

^2J(H,H) of ~13 Hz are assigned to the benzylic protons 9. These six resonances originate from three pairs of diastereotopic protons (intensity ratio 1:1:1), as has been established by a 2D H,H COSY spectrum. Those belonging to a pair are denoted as protons 9′A, 9′B and 9″A, 9″B, as has been used previously in Figures 3 and 4. The doublets of the NH_2 protons (10″A, 10″B and so on) are slightly broadened. These aniline proton signals are marked by oblique lines in Figure 9. From their intensity ratio and a 2D H,H COSY spectrum, it is established that these signals are also assignable to pairwise diastereotopic protons. One pair 10′A, 10′B exhibits a degeneracy which is partially lifted at 283 K. The splitting pattern is characteristic for a strongly coupled {AB} spin system.

Polarization transfer experiments at 273 K established that the proton signals 9′B, 9″B, 9‴B must be assigned to three equatorial protons of the benzyl groups in the six-membered chelate rings (Chart 2 and Table 1). Irradiation into the degenerate signal at δ = 5.40 (10′A, 10′B) results in a NOE amplification of the resonance at δ = 4.65 (9′A). This proves that this is a genuine signal of complex **2** and does not arise from an adventitious impurity. Furthermore, the observed magnetization transfer between protons 9′A and 9′B and between protons 9″A and 9‴A shows that on the NMR time scale slow exchange processes occur even at 273 K.

These observations conclusively prove that in solution all three six-membered chelate rings in complex **2** are not equivalent (C_1 symmetry). Therefore in the aromatic region three {ABCD} spin systems are anticipated. The same is true for the ethylene bridge protons 7 and 8 of the 1,4,7-triazacyclononane backbone of **2**, which resonate in the region 1.5−3.5 ppm with the small difference that the multiplets of the individual protons of the latter group are broader due to a larger

(23) Günther, H. *NMR-Spektroskopie*, 2nd ed.; Georg Thieme Verlag: Stuttgart, Germany, 1983; p 229.

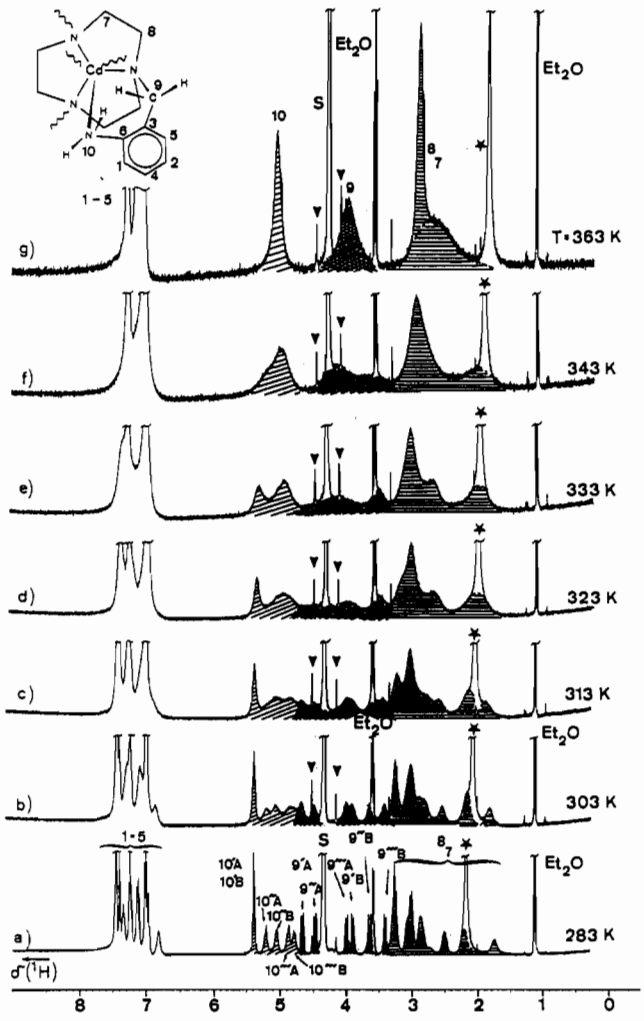

Figure 9. Variable-temperature 400 MHz ^{1}H NMR spectra of **2** in nitromethane-d_3 solution. The asterisks denote water signals; black triangles denote ^{13}C satellites of solvent signals. The primed indices, e.g. 10′A, 10″A, and 10‴A, indicate a given H atom in the different six-membered chelate rings irrespective of the actual conformation (for atom labeling see Chart 2).

J(H,H) coupling. This leads to even more complicated signal patterns. In Figure 9 the ethylene proton signals are marked with horizontal lines.

From variable-temperature measurements (Figure 9, traces a–g), coalescence of the following signal groups could be followed: NH_2 protons 10A, 10B, benzylic protons 9A, 9B, and ethylene protons 7 and 8. The spectrum of **2** at 363 K (Figure 9, trace g) is quite similar to that of **1** at room temperature. A detailed line shape analysis and a determination of $\Delta G^{\ddagger}$ have not been possible due to overlaps with other proton signal groups and signals of the respective solvent. Nevertheless, it is clear that complex **2** in solution displays three intramolecular dynamic processes of similar or equal activation barriers: (i) a pseudorotation converting the Λ configuration into Δ which is accompanied (ii) by $(\lambda\lambda\lambda) \rightleftharpoons (\delta\delta\delta)$ interconversion of the five-membered chelate rings and (iii) by boat $\rightarrow$ twist-boat inversion of the six-membered chelate rings.

Investigation of the dynamics of complex **3** in solution has not been possible due to the low solubility (even in nitromethane-d_3) of this species. The ^{1}H NMR spectrum at 363 K shown in Figure 6 (trace c) is quite similar to that of the zinc complex **1** at the same temperature. ^{13}C NMR spectra of **3** at 363 and 273 K (both not shown) are similar to those of **2** (see Table 2).

In summary, the solid state structures of the respective dications of complexes **1**–**3** have been firmly established by X-ray crystallography and solid state CP/MAS ^{13}C NMR spectroscopy to possess C_1 symmetry. In contrast, in solution all three complexes are dynamic. Three different processes are observed: (i) $\Lambda \rightleftharpoons \Delta$ interconversion of the MN_6 polyhedra, (ii) $(\lambda\lambda\lambda)_5 \rightarrow (\delta\delta\delta)_5$ inversion of the three five-membered chelate rings $\overbrace{M-N_{amine}-C-C-N_{amine}}$ (and vice versa), and (iii) twist-boat $\rightarrow$ boat inversion of the six-membered chelate rings. For the zinc complex **1**, the C_1 structure is not frozen out even at the lowest experimentally available temperature of 203 K whereas, for **2** and (probably) **3**, this asymmetric structure is clearly present. Conversely, at the highest experimentally available temperature of 363 K, an averaged C_3 structure is only observable for **1** on the NMR time scale whereas for **2** and **3** this limit has not yet been reached. Since it has also been shown by NMR spectroscopy for **3** that in the temperature range 203–363 K all six nitrogen donor atoms are coordinated to the divalent metal Hg^{2+} (i.e., no M–N dissociation is detectable), we propose that the $\Lambda \rightleftharpoons \Delta$ interconversion occurs via a Bailar twist. As the twist angle ϑ is the smallest for **1** and somewhat larger for **2** and **3**, it would appear that the activation energy $\Delta G^{\ddagger}$ is the smallest for **1** and somewhat larger for **2** and **3**.

Acknowledgment. We thank the Fonds der Chemischen Industrie for financial support of this work.

Supporting Information Available: Listings of full details of the structure determinations, atom coordinates, bond distances and angles, anisotropic thermal parameters, and H atom positions of [ZnL]-$(ClO_4)_2 \cdot 0.5H_2O$, [CdL]$(ClO_4)_2 \cdot 0.5H_2O$, and [HgL]$(ClO_4)_2 \cdot 0.5H_2O$ (27 pages). Ordering information is given on any current masthead page.

IC950684P